Research Article

Photonic Heterodyne Pixel for Imaging Arrays at Microwave and MM-Wave Frequencies

Á. R. Criado,[1] J. Montero-dePaz,[2] C. de Dios,[1] L. E. García,[2] D. Segovia,[2] and P. Acedo[1]

[1] *Electronics Technology Department, Universidad Carlos III de Madrid, 28911 Leganés, Spain*
[2] *Grupo de Radiofrecuencia (GRF), Universidad Carlos III de Madrid, 28911 Leganés, Spain*

Correspondence should be addressed to P. Acedo, pag@ing.uc3m.es

The use of photonic heterodyne receivers based on semiconductor optical amplifiers to be used in imaging arrays at several GHz frequencies is evaluated. With this objective, a 3×3 imaging array based on such photonic pixels has been fabricated and characterized. Each of the receiving optoelectronic pixels is composed of an antipodal linear tapered slot antenna (LTSA) that sends the received RF signal directly to the electrical port of a semiconductor opticalamplifier (SOA) acting as the optoelectronic mixer. Both the local oscillator (LO) and the intermediate frequency (IF) signals are directly distributed to/from the array pixels using fiber optics, that allows for remote LO generation and IF processing to recover the image. The results shown in this work demonstrate that the performances of the optoelectronic imaging array are similar to a reference all-electronic array, revealing the possibility of using this photonic architecture in future high-density, scalable, compact imaging arrays in microwave and millimeter wave ranges.

1. Introduction

Microwave photonics and radio-over-fiber (RoF) techniques have been used in antenna arrays for some years now typically associated with local oscillator (LO) distribution and remote intermediate frequency (IF) processing [1]. The advantages usually associated with the use of such techniques are the high bandwidth capabilities, the electromagnetic interference (EMI) immunity, the extremely low transmission losses when using optical fibers, and the possibilities of including signal processing features, like true local time delay (TTD) [2] or optical beam forming [3]. Their advantages are also associated with the availability of optical/photonic devices in the telecom wavelength range which, due to the growth of the optical communications in the last decades, provide us with high-performance, wide-variety, compact, and low-cost (COTS) optical components suitable for its use in microwave photonics and RoF.

Following this trend, new functionalities based on photonic processing of RF are becoming available to be incorporated into arrays beyond optical signal distribution. In this sense, a major contribution to obtain high-density

receiving arrays based on photonic techniques would be the obtaining of a photonic heterodyne receiver able to perform directly the mixing of the LO (photonically distributed) and the received RF with high sensitivity. This all-optical pixel would reduce the several electrooptical (EO) conversions typical to conventional RoF systems and would be able to be integrated directly into the mature optical signal distribution architectures already available. In order to obtain such heterodyne optoelectronic RF detector, several mixing techniques have been already proposed using components as Mach-Zehnder modulators [4], electroabsorption modulators [5], or dual-mode monolithic laser sources [6] that show polarization dependence or low conversion efficiencies. Recently, semiconductor optical amplifiers (SOAs) have also been proposed as optoelectronic mixers [7–10]. Optical mixing using SOAs has been demonstrated both in all-optical [9, 10] and electrooptical (EO) configurations [7, 8]. In the EO approach, which is the most interesting in terms of obtaining a photonic heterodyne mixer, one of the electrical signals involved (i.e., the local oscillator (LO) or the radiofrequency (RF)) is modulated onto an optical carrier that is delivered to the optical input of the SOA. The other electrical

signal is directly applied to the electrical port of the SOA modulating its bias voltage. Both downconversion [8] and upconversion [7] have been reported.

One of the fields these all-optical pixel-based receiving arrays will have a great impact on is microwave and millimeter wave imaging. These techniques have been successfully demonstrated for a variety of applications like nondestructive testing [11], medical imaging [12], and security applications [13]. Usually these systems, working either in near field or far field, have their pixel elements multiplexed in the RF level into a single receiver to obtain reasonable size systems. Recently, a portable real-time camera at 24 GHz based on this strategy has been reported [14], but although the speed is reasonably good (22 frames per second) the resolution (24×24 pixels) is still far to be the required for the applications mentioned above, especially if we address the necessity of obtaining a portable (low-size and -weight) device.

In this sense, the incorporation of all-optical RF receiving pixel-based photonic mixing techniques [15] to imaging arrays will have a major impact on the resulted size, weight, and power consumption of the system. The high integration potential associated to PICs (photonic integrated circuits) [16] allows also for the integration on the same substrate of all the required functionalities necessary to process RF frequencies in the optical domain. Nowadays, several high-functionality PICs have already been reported [17], especially for optical communication purposes, demonstrating that the technology is already mature to implement other functionalities.

With this aim, in this work we present a three by three element (3×3) imaging array based on a heterodyne optoelectronic pixel based on an electrooptical (EO) ultra nonlinear mixer using an ultra nonlinear semiconductor optical amplifier (XN-SOA) [15]. This XN-SOA EO mixer presents a direct RF electrical input provided by an antipodal linear tapered slot antenna (LTSA) [18]. The LO is optically introduced at the optical input of the XN-SOA, and the IF is also optically delivered at its output, allowing for remote photonic LO generation and remote IF processing over optical fiber. Both, the mixing scheme and the used antenna make up a compact, low-cost, and flexible receiving heterodyne antenna that offers good scalability properties for imaging array applications. In this work, first imaging results using the heterodyne optoelectronic pixel 3×3 array are presented. Although the imaging system presented in this paper works at a relatively low frequency (13 GHz), the high bandwidth associated to the photonic components already available for optical communications opens the possibility to scale the presented architecture to higher (millimeter wave) frequencies.

2. Description and Characterization of the Heterodyne Optoelectronic Pixel for Imaging Arrays

2.1. Heterodyne Optoelectronic Pixel Fundamentals.
The core of the reported photonic imaging array is an ultra nonlinear

semiconductor optical amplifier (XN-SOA) based heterodyne pixel receiver that makes our system compact and cost-effective. The scheme is depicted in Figure 1 [15]. The LO signal (f_{LO}) is applied to a distributed feedback (DFB) diode laser (QPhotonics QDFBLD-1550-50) that works under gain switching conditions [19], allowing for the modulation of the optical carrier without external modulators. The photonic LO produced has an optical frequency comb-like spectra [15] that is distributed to the heterodyne receiver using a fiber link (Figure 1(a)). The LO is then coupled to the optical input of the ultra nonlinear SOA (CIP SOA-XN-OEC-1550), where the EO mixing process takes place when the RF electrical signal (f_{RF}) introduced into the electrical port of the XN-SOA modulates its bias point. The XN-SOA device has a small signal gain of 20 dB at 150 mA bias current and a maximum saturated optical output power of 13 dBm. The obtained IF appears modulating the optical carrier at the output of the XN-SOA (Figure 1(c)) and is recovered at the end of the optical downlink using a high bandwidth photodiode (u2t XPDV2120R) followed by a low-pass filter. This scheme is cost-effective and takes advantage of the additional nonlinearities of the mixer and its polarization independence compared to other schemes already proposed [7, 8].

It is important to note in this scheme that no external modulator is used for the photonic LO generation and neither a laser nor an external modulator is needed for modulating the RF signal onto an optical carrier for the mixing process. Moreover, no optical coupler is required to add the optical signals containing LO and RF prior to the SOA input, as it is typical to previous reported schemes [9]. In this way, most devices usually employed in typical RoF architectures are avoided, thus having a much more compact and cost-effective configuration, allowing for easier integration onto a single PIC. The proposed approach, with the LO and the IF distributed over fiber, results in an especially suitable strategy for scaled and flexible signal distribution in large array applications.

2.2. Heterodyne Optoelectronic Pixel Description.
The optoelectronic heterodyne pixel incorporates to the EO mixing scheme described above for heterodyne RF detection, a broadband antenna to provide the XN-SOA with an impedance as constant as possible along its broad working band. For this reason an antipodal linear tapered slot antenna (LTSA) [18] has been selected (Figure 2). As a substrate, Rogers Duroid 5880, with $\varepsilon r = 2.2$ and 0.787 mm thickness, has been chosen. In Figure 2, we see how the antenna collects the RF signal that is directly delivered to the bias port of the XN-SOA of Figure 1. The optical signal at the output of the XN-SOA, that contains the IF, is delivered over optical fiber to the remote IF-processing stage, where a photodiode performs the conversion from optical to electrical domain.

2.3. Heterodyne Optoelectronic Pixel Characterization.
The characterization of the heterodyne pixel must include both the evaluation of the performances of the photonic mixing scheme (Figure 1) and the antenna (Figure 2). The parameter
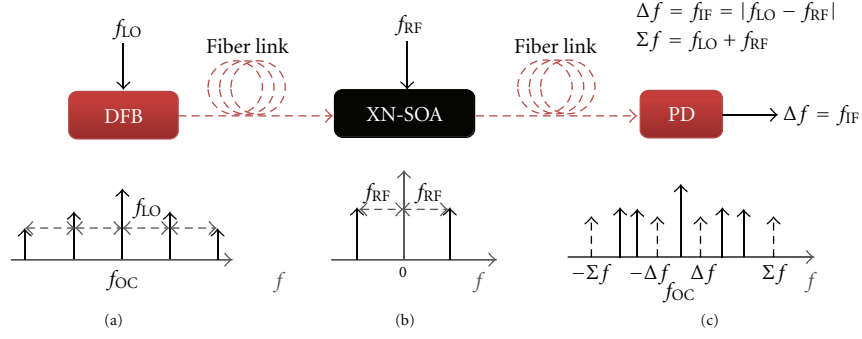
FIGURE 1: EO mixing concept using an ultra nonlinear SOA. (a) Optical output of GS DFB laser; (b) electrical signal modulating the XN-SOA bias; (c) optical output of the XN-SOA (only sum and difference terms are represented).
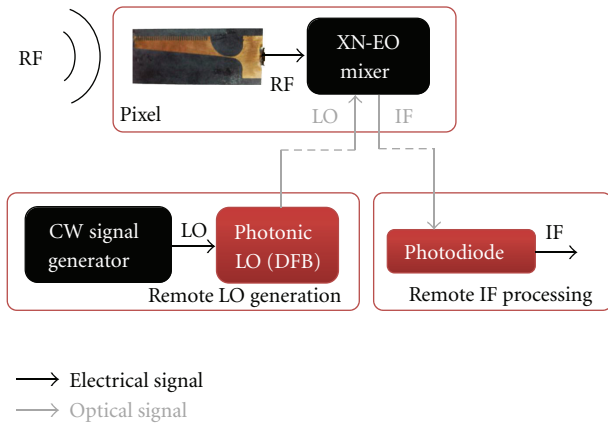

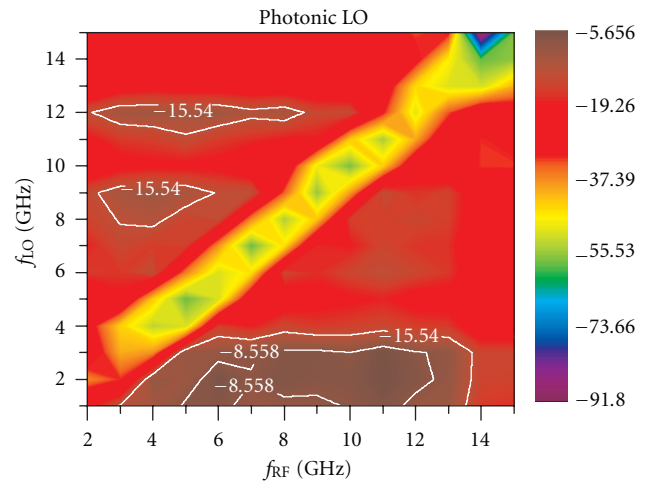FIGURE 2: Heterodyne photonic receiving antenna setup.

FIGURE 3: Downconversion ratios in dB for the photonic mixer. Contour lines represent 3 dB and 10 dB bandwidth.

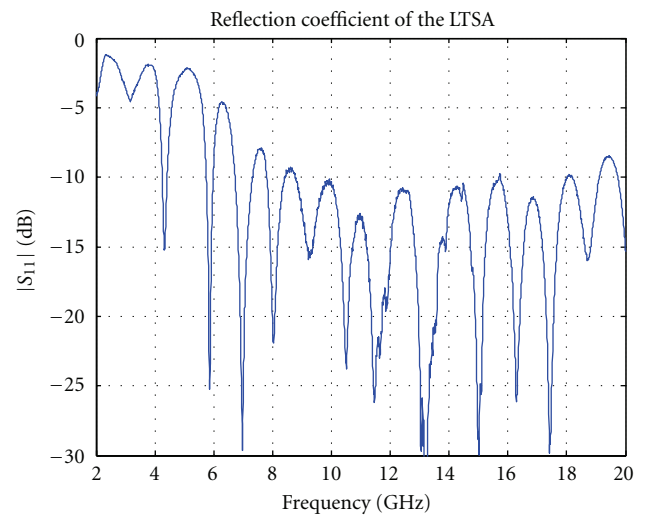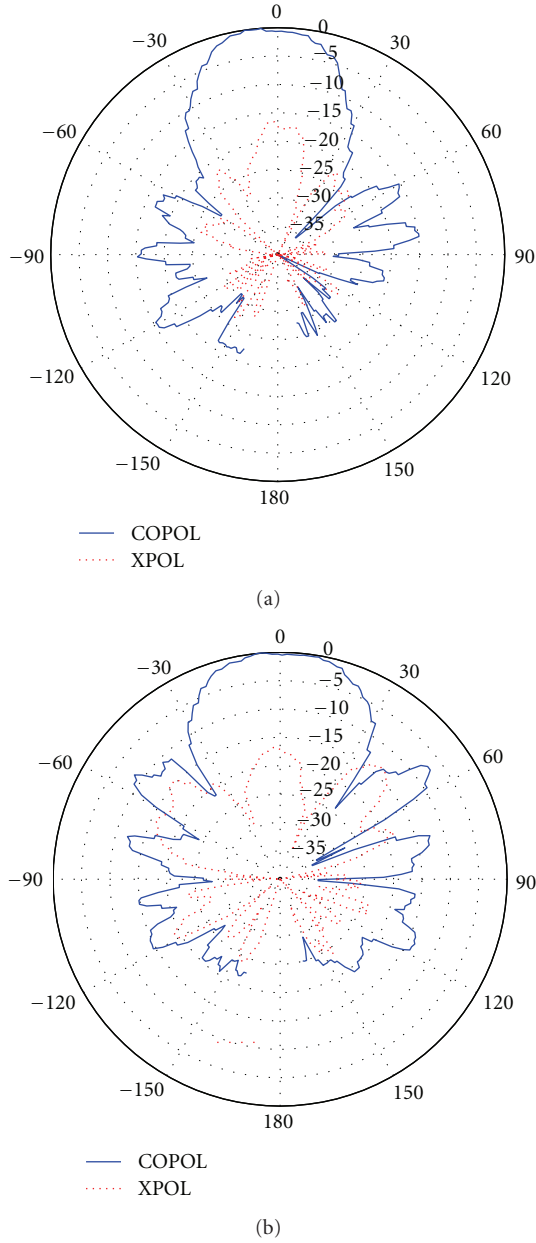FIGURE 4: Measured reflection coefficient of the manufactured LTSA.

we have used to evaluate the performance of the photonic mixer has been the downconversion ratio (Figure 3), defined for optoelectronics mixers as the ratio between the electrical power of the downconverted signal at f_{IF} (output of the photodiode) and the electrical power of the RF signal present after mixing at f_{RF} [9]. An analysis of the frequency dependence of the downconversion ratio has been performed sweeping both f_{LO} and f_{RF} up to 15 GHz. The bias current applied to the DFB is 40 mA, for an average optical power around 5 mW. The XN-SOA is biased at 150 mA (saturation) and shows an average optical output power of 10 mW. The regions with better (higher) conversion ratios appear for RF frequencies in the ~4 to 13 GHz range and LO frequencies below 4 GHz. When both frequencies (LO and IF) are close to each other, the conversion ratio falls as expected (homodyne operation).

As mentioned before, the broadband antenna design selected for the receiver pixels is an antipodal LTSA [18] that includes a number of corrugations in order to make the beam symmetric and improve its radiation pattern [20]. The characterization of the antenna started with the measurement of the reflection coefficient. In Figure 4, we show the reflection coefficient for the LTSA demonstrating a working frequency band from 7 GHz to 20 GHz with the

COPOL
XPOL

(a)

Figure 6: 3 × 1 Subarray based on antipodal LTSAs.

COPOL
XPOL

(b)

Figure 5: Antipodal LTSA radiation pattern (measured at 13 GHz).

Figure 7: Picture of the actual 3 × 3 array inside the anechoic chamber.

desired relatively constant impedance presented to the XN-SOA over frequency. Also the radiation pattern has been measured, as shown in Figure 5, where such radiation pattern at 13 GHz is displayed as an example of how each of the elements of the array radiates. This antenna has a directivity in the whole band around 9 dBi-10 dBi.

3. Imaging Array Description and Experimental Setup

The final objective of this work is to validate the use of the introduced optoelectronic pixel for heterodyne RF detection in imaging arrays incorporating the advantages of remote
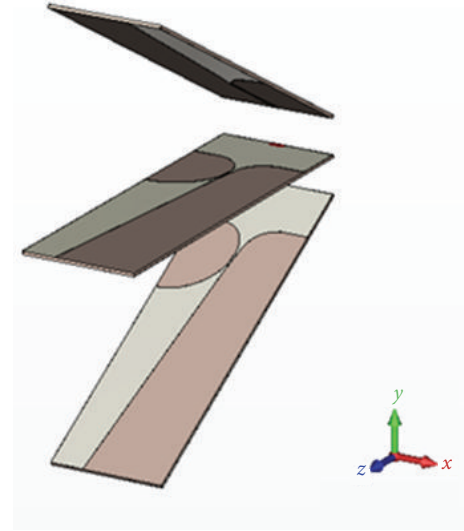
photonic LO and IF distribution and the high integration capability of photonic circuits. For this reason, a 3 × 3 element array has been designed and fabricated based on the pixel described above to proof the concept. The 3 × 3 array design is based on three 3 × 1 subarray elements as shown in Figure 6, where we can see the LTSA radiant elements chosen for the pixels. Upper and lower elements are tilted 30° with respect to the central element in order to scan different directions and provide faster scanning capabilities. The final array built is shown in Figure 7, where we can see the actual appearance of the array made of the subarrays of Figure 5. A 130 × 110 × 70 mm PVC box has been designed to hold the complete array and provide the desired tilt to the antennas. Each horizontal subarray (Figure 6) is formed by 3 LTSAs printed on a 110 × 100 mm Rogers Duroid 5880 substrate separated 30 mm from each other. Each subarray
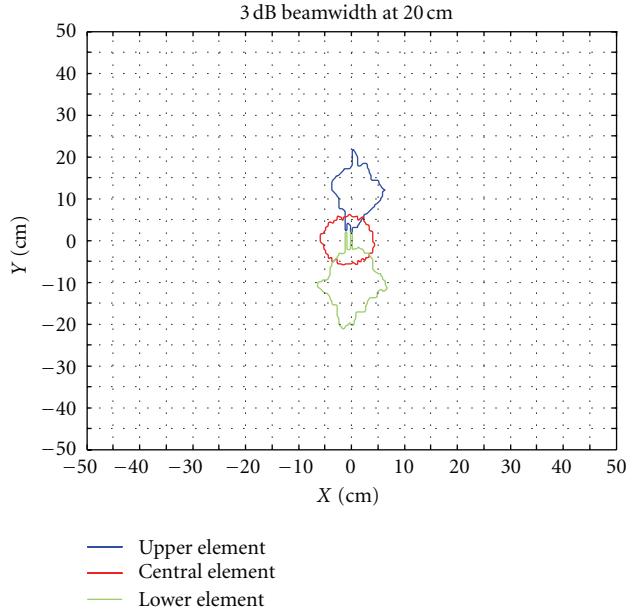
FIGURE 8: Beam spot diameter at 20 cm from the subarray from Figure 6. Working frequency 13 GHz.
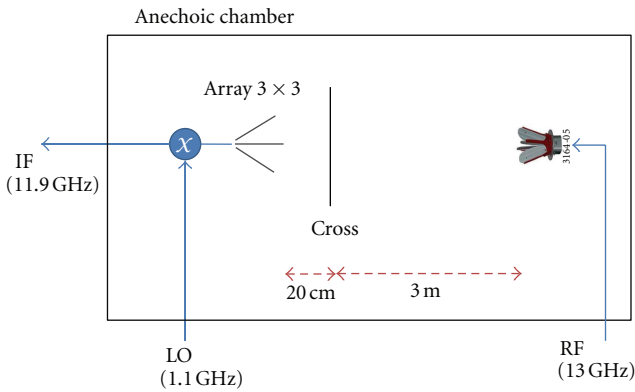

FIGURE 9: Imaging experiment (see text for details).

FIGURE 10: Metallic target for the imaging experiment.

has been manufactured with a LPKF ProtoLaser S laser milling machine.

As mentioned briefly in the introduction, microwave imaging arrays (cameras) can be operated either in near field (higher spatial resolution) or far field. If the later is the case (far field imaging), the spatial resolution is fixed by the spot size of the array elements individual beams. In Figure 8, we show the measured spot diameter for the subarray shown in Figure 6 at 20 cm of the antenna (inside an anechoic chamber). These measurement results show 10 cm spot diameters (3 dB) for 13 GHz RF frequency. It is important to highlight that this spot diameter for the antenna elements that fixes the spatial resolution of the imaging system can be improved by increasing the operating frequency, as the types of antennas we are planning to use at higher frequencies present similar radiation patterns. In this situation, it is basically the operation frequency the
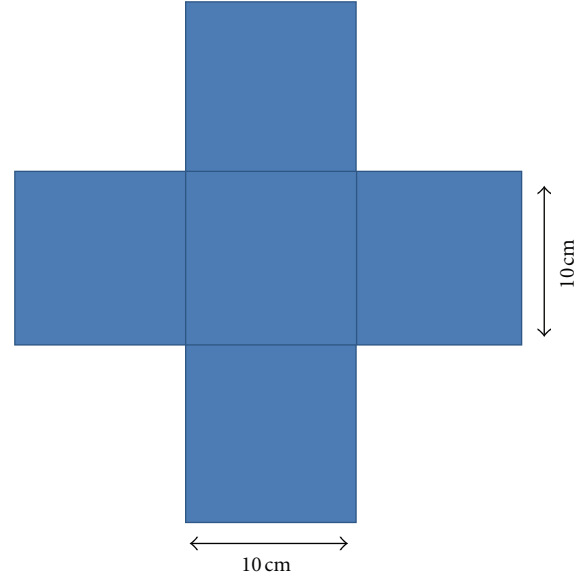
parameter that fixes the spatial resolution of the system (beam diameter).

In order to evaluate the imaging performances of the array, an imaging experiment has been carried out (Figure 9). The working frequency has been chosen using the down-conversion ratios map of Figure 3 for optimum performance of the heterodyne photonic pixels (f_{RF} = 13 GHz, f_{LO} =1.1 GHz). The 11.9 GHz IF (intermediate frequency) is remotely recovered for each pixel with a high-speed photo-diode). In Figure 9, we can see how a transmitter element (horn) illuminates at the designated frequency (13 GHz) a metallic object placed 3 m from the emitter (horn) and 20 cm from the 3×3 imaging array. It is important to note here that these are the conditions used to evaluate the spot diameter for the independent elements of the array (10 cm, Figure 8), which will limit the spatial resolution of the system. For the results shown in the next section, the metallic object chosen for the imaging experiment is an aluminum cross of 300 mm × 300 mm dimensions shown in Figure 10. Its dimensions are in the order of magnitude of the beam size.

4. Experimental Results

The images obtained for the object of Figure 10 are shown in Figures 11 and 12 using two different receiving pixels. As a preliminary step, and to separate the influence of the use of an optoelectronic pixel from the actual imaging capabilities of the array built, the array for Figure 7 is equipped with a set of electronic mixers, including RF preamplification, to evaluate the actual spatial resolution of the array. The results obtained are shown in Figure 11, where we can see that the cross is resolved through the simultaneous recovery of the amplitude signals for each pixel of the array. In this sense, it is important to note again that the beam diameter at 20 cm of the array is 10 cm, limiting the spatial resolution as can be extracted from Figure 11.
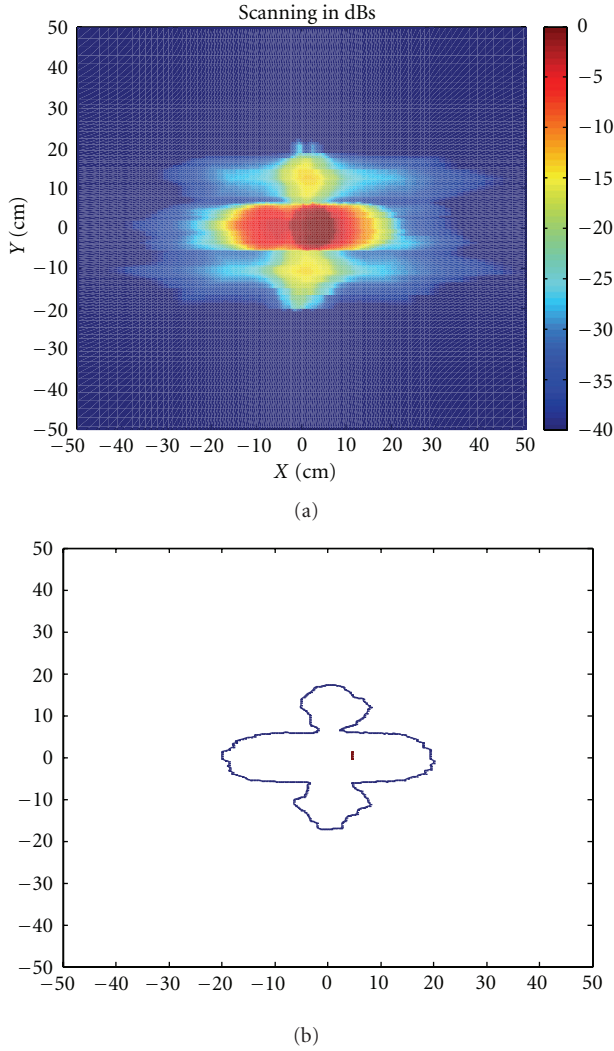
(a)

(b)

Figure 11: Results from the scanning of the object shown in Figure 10 with the 3×3 array using an electronic mixer for heterodyne detection. (a): power difference measured for each pixel with and without the cross (in dB). (b): -10 dB contour for the results shown on (a).

The scanning results obtained for the optoelectronic heterodyne pixel array are shown in Figure 12. We can observe that the image obtained is similar to the one recovered using electronic pixels (Figure 11). It must be noted at this point that, in this case, both the LO and IF are optically distributed using fiber optics to/from the array, eliminating the necessity of further electronics in the individual pixels. In this sense, this photonic-based imaging array presents evident advantages associated with its lower weight, lower power consumption EMI immunity, and flexibility, along with the integration capabilities associated with the possibility of implementing the XN-SOA and optical distribution fibers as photonic integrated circuits.

5. Conclusions

Microwave and millimeter wave imaging techniques have demonstrated their capacities in several and important
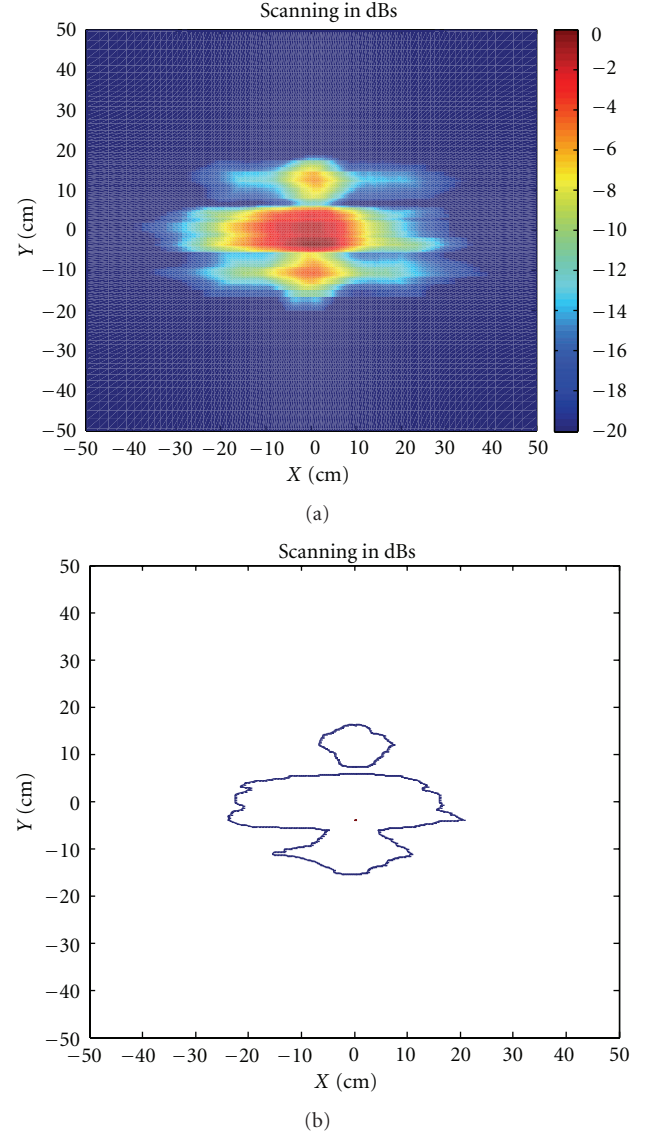

(a)

(b)

Figure 12: Results from the scanning of the object shown in Figure 10 with the 3×3 array using an optoelectronic mixer for heterodyne detection with remote LO and IF distribution. (a): power difference measured for each pixel with and without the cross (in dB). (b): -10 dB contour for the results shown on (a).

application fields. In order to introduce the well-known advantages of microwave photonics and radio-over-fiber techniques in this emerging field, in this work we have designed, implemented, and tested an imaging array based on a photonic heterodyne receivers. The objective is to take advantage of the already well-known advantages of photonic local oscillator distribution in antenna arrays and the introduction of a novel optoelectronic mixer to reduce even further the electronic components count at the antenna front-end, reducing thus power consumption, space, and cost at the expenses of a little less sensitivity. The photonic setup chosen, based on an XN-SOA in EO configuration, reduces also the optical elements typical to other optoelectronic mixers schemes (using external modulators, polarization control optics, etc), allowing for further

integration of the different optoelectronic components in photonic integrated circuits (PICs).

The results shown demonstrate the possibility of using this approximation for imaging arrays in the GHz band, but, even more important, they open the possibility to scale this architecture (once that has been validated) to higher frequencies (100 GHz). This further step is associated with the high bandwidth of the photonic components already available in the market for optical communications. In this sense, preliminary work of 100 GHz imaging arrays are already being under development.

References

[1] J. Marti and J. Capmany, "Microwave photonics and radio-over-fiber research," *Microwave Magazine, IEEE*, vol. 10, pp. 96–105, 2009.

[2] P. Berger, J. Bourderionnet, F. Bretenaker, D. Dolfi, and M. Alouini, "Time delay generation at high frequency using SOA based slow and fast light," *Optics Express*, vol. 19, pp. 21180–21188, 2011.

[3] L. Jofre, C. Stoltidou, S. Blanch et al., "Optically beamformed wideband array performance," *IEEE Transactions on Antennas and Propagation*, vol. 56, no. 6, pp. 1594–1604, 2008.

[4] T. Kuri, H. Toda, and K. I. Kitayama, "Dense wavelength-division multiplexing millimeter-wave-band radio-on-fiber signal transmission with photonic downconversion," *Journal of Lightwave Technology*, vol. 21, no. 6, pp. 1510–1517, 2003.

[5] B. Hraimel, X. Zhang, and K. Wu, "Photonic down-conversion of millimeter wave multiband orthogonal frequency division multiplexing ultra-wideband using four wave mixing in an electro-absorption modulator," *Journal of Lightwave Technology*, vol. 28, no. 13, Article ID 5473097, pp. 1987–1993, 2010.

[6] P. Acedo, H. Lamela, and C. Roda, "Optoelectronic up-conversion using compact laterally mode-locked diode lasers," *IEEE Photonics Technology Letters*, vol. 18, no. 17, pp. 1888–1890, 2006.

[7] J. Palací, G. Villanueva, and J. Herrera, "EAM-SOA millimeter-wave frequency up-converter for radio-over-fiber applications," *Optics Communications*, vol. 284, no. 1, pp. 98–102, 2011.

[8] C. Bohémond, A. Sharaiha, T. Rampone, and H. Khaleghi, "Electro-optical radiofrequency mixer based on semiconductor optical amplifier," *Electronics Letters*, vol. 47, no. 5, pp. 331–333, 2011.

[9] J. H. Seo, C. S. Choi, Y. S. Kang, Y. D. Chung, J. Kim, and W. Y. Choi, "SOA-EAM frequency up/down-converters for 60-GHz Bi-directional radio-on-fiber systems," *IEEE Transactions on Microwave Theory and Techniques*, vol. 54, no. 2, pp. 959–966, 2006.

[10] C. Bohémond, P. Morel, A. Sharaiha, T. Rampone, and B. Pucel, "Experimental and simulation analysis of the third-order input interception point in an all-optical rf mixer based on a semiconductor optical amplifier," *Journal of Lightwave Technology*, vol. 29, no. 1, Article ID 5638116, pp. 91–96, 2011.

[11] S. Kharkovsky and R. Zoughi, "Microwave and millimeter wave nondestructive testing and evaluation," *IEEE Instrumentation and Measurement Magazine*, vol. 10, no. 2, pp. 26–38, 2007.

[12] T. Henriksson, N. Joachimowicz, C. Conessa, and J. C. Bolomey, "Quantitative microwave imaging for breast cancer detection using a planar 2.45 GHz system," *IEEE Transactions on Instrumentation and Measurement*, vol. 59, no. 10, pp. 2691–2699, 2010.

[13] D. M. Sheen, D. L. McMakin, and T. E. Hall, "Three-dimensional millimeter-wave imaging for concealed weapon detection," *IEEE Transactions on Microwave Theory and Techniques*, vol. 49, no. 9, pp. 1581–1592, 2001.

[14] M. T. Ghasr, M. A. Abou-Khousa, S. Kharkovsky, R. Zoughi, and D. Pommerenke, "Portable real-time microwave camera at 24 GHz," *IEEE Transactions on Antennas and Propagation*, vol. 60, no. 2, pp. 1114–1125, 2012.

[15] Á. R. Criado, C. de Dios, and P. Acedo, "Characterization of Ultra Non Linear SOA in a heterodyne detector configuration with remote Photonic Local Oscillator distribution," *IEEE Photonics Technology Letters*, vol. 24, no. 13, pp. 1136–1138, 2012.

[16] X. Leijtens, "JePPIX: the platform for Indium Phosphide-based photonics," *Optoelectronics, IET*, vol. 5, pp. 202–206, 2011.

[17] S. Ristic, A. Bhardwaj, M. Rodwell, L. Coldren, and L. Johansson, "An optical phase-locked loop photonic integrated circuit," *Journal of Lightwave Technology*, vol. 28, no. 4, pp. 1–1, 2009.

[18] K. S. Yngvesson, T. L. Korzeniowski, Y. S. Kim, E. L. Kollberg, and J. F. Johansson, "Tapered slot antenna—a new integrated element for millimeter—wave applications," *IEEE Transactions on Microwave Theory and Techniques*, vol. 37, no. 2, pp. 365–374, 1989.

[19] C. De Dios and H. Lamela, "Improvements to long-duration low-power gain-switching diode laser pulses using a highly nonline optical loop mirror: theory and experiment," *Journal of Lightwave Technology*, vol. 29, no. 5, Article ID 5678610, pp. 700–707, 2011.

[20] J. B. Rizk and G. M. Rebeiz, "Millimeter-wave Fermi tapered slot antennas on micromachined silicon substrates," *IEEE Transactions on Antennas and Propagation*, vol. 50, no. 3, pp. 379–383, 2002.